

The order parameter symmetry of doped $\text{YBa}_2\text{Cu}_3\text{O}_7$

This article has been downloaded from IOPscience. Please scroll down to see the full text article.

1998 J. Phys.: Condens. Matter 10 10621

(<http://iopscience.iop.org/0953-8984/10/47/013>)

View [the table of contents for this issue](#), or go to the [journal homepage](#) for more

Download details:

IP Address: 171.66.16.210

The article was downloaded on 14/05/2010 at 17:56

Please note that [terms and conditions apply](#).

The order parameter symmetry of doped $\text{YBa}_2\text{Cu}_3\text{O}_7$

P K Mohanty^{†§} and A Taraphder^{†‡||}

[†] Mehta Research Institute, Jhusi, Allahabad 221506, India

[‡] Department of Physics & Meteorology and Centre for Theoretical Studies, Indian Institute of Technology, Kharagpur 721302, India

Received 13 May 1998, in final form 10 September 1998

Abstract. A two-band model that reproduces the Fermi surface seen in angle-resolved photo-emission experiments is used to study the symmetry of the order parameter of doped $\text{YBa}_2\text{Cu}_3\text{O}_7$. The model incorporates the effects of tunnelling in the c -direction between the planes and chains in YBCO. It is observed that a suitable choice of the phases of the symmetric pair wave-function in the planes and chains leads to both s - and d -wave-like features. We calculate the mean-field phase diagram of this system, observe the shift in the position of the node(s) of the order parameter(s) on the Fermi surface with doping and try to reconcile the seemingly contradictory experimental observations as regards the presence of features that resemble s -wave and/or d -wave symmetry. The effect of the leading-order, two-dimensional fluctuations on the mean-field transition temperature is shown to be small.

1. Introduction

The nature of the symmetry of the order parameter (OP) for the high- T_c cuprates has occupied centre stage in high- T_c research of late. An understanding of this would shed considerable light on the microscopic interactions that lead to superconductivity in these unusual systems. Broadly speaking, there are four different classes of experiments that probe the symmetry of the OP.

(i) Transport and thermodynamic measurements, notably of the temperature dependence of the penetration depth (λ) [3], which show a linear temperature dependence of λ , indicate that at low energies the density of superconducting states (SDOS) varies linearly with energy in pure samples, a signature of gapless excitations.

(ii) ARPES experiments [4], which show a node (with a small offset) along the (π, π) direction of the Fermi surface (FS) of $\text{YBa}_2\text{Cu}_3\text{O}_7$.

(iii) Josephson measurements: the magnetic field dependence observed in dc SQUIDS [5, 6] predicts a π phase shift consistent with the d -wave scenario. Conversely, c -axis Josephson tunnelling [7] between twinned and untwinned $\text{YBa}_2\text{Cu}_3\text{O}_7$ and a Pb junction finds a Josephson current, though small, indicative of a symmetric OP. The critical current between a hexagonal grain and its surroundings is found to be non-zero [8] and to scale with the number of sides engaged, consistently with the presence of a conventional s -wave component.

[§] E-mail: peekay@mri.ernet.in.

^{||} E-mail: arghya@iitkgp.ernet.in, arghya@mri.ernet.in.

(iv) The sensitivity of the superconducting transition temperature to elastic scattering is too weak (it obeys, instead, the Ioffe–Regel criterion, $k_f l = 1$) to conform to the behaviour of a pure d-wave symmetry [9].

Importantly, YBCO is orthorhombic and not tetragonal; an admixture of s and d components is thus unavoidable [10]. It thus appears that the existence of a node on the FS is more or less established; what is not agreed upon yet is its origin.

In view of this conflict, it is useful to look for models that (a) incorporate the essence of the band structure of the system concerned and (b) reproduce many of the experimentally observed features. A model for studying superconductivity in two coupled bands was used earlier by Suhl *et al* [11]. Recently a similar model has been used by Combescot and Leyronas [12]. We study the model in detail and show that it is indeed possible to reproduce many of the observed features of the OP without explicitly considering a d-wave pairing function, and that features consistent with both d and s waves are obtainable with a suitable choice of the relative phase of two isotropic pairing functions residing primarily on the plane- and chain-derived bands.

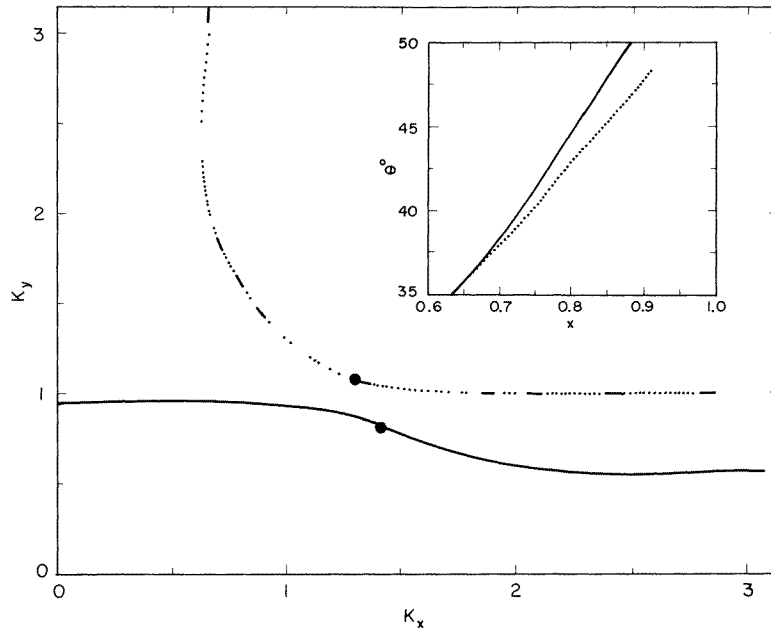


Figure 1. The two sheets of the FS are shown in the first quadrant of the BZ. The dotted (solid) line corresponds to $\epsilon^- = 0$ ($\epsilon^+ = 0$). The filled circles show the positions of the nodes of the OP on the FS for $x = 0.9$. The variations of the node positions on the FS with doping (x) are shown in the inset.

2. The model, calculations and results

We consider the following Hamiltonian: $H = H_0 + H_I$, where

$$H_0 = \sum_{k\sigma} [\epsilon_k c_{k\sigma}^\dagger c_{k\sigma} + \epsilon'_{k_y} d_{k_y\sigma}^\dagger d_{k_y\sigma} + t(d_{k_y\sigma}^\dagger c_{k\sigma} + \text{HC})]. \quad (1)$$

ϵ_k and ϵ'_{k_y} are energy dispersions, and $c_{k\sigma}$, $d_{k\sigma}$ are annihilation operators for electrons in the plane and the chain respectively. The interband term t is known to be small ($t \approx 50$ meV) [13]; it introduces interband interaction and is assumed momentum independent. This implies that in the YBCO system, an electron is never in a true eigenstate of either the planes or the chains; it has components in both of the bands. In order to fit our band structure with a realistic one obtained from the ARPES data [1, 4] for the YBCO system, we take five nearest-neighbour hopping parameters in the plane and two nearest neighbours in the chain, in the same spirit as in the work of Fehrenbacher and Norman [14], where a six-parameter fit is used for the ARPES data for the Bi-2212 system. The FS thus obtained and shown in figure 1 consists of two sheets: a nearly non-dispersive one-dimensional band and a typical two-dimensional band, nearly non-dispersive along the two symmetry directions. The Fermi surface very closely resembles the observed FS [4] including the position of the van Hove singularity (figure 2) (about 10 meV away from the FS [15]) seen in $\text{YBa}_2\text{Cu}_3\text{O}_7$, with the following choice of the parameters: $\{t_1, \dots, t_5\} = \{300, 100, 25, 25, 20\}$ meV and $\{h_1, h_2\} = \{530, 135\}$ meV.

The quadratic part of the Hamiltonian H_0 can be diagonalized by the introduction of quasiparticle operators α_k and β_k defined by

$$\begin{pmatrix} c_{k\sigma} \\ d_{k\sigma} \end{pmatrix} = \begin{pmatrix} \frac{t}{\sqrt{t^2 + (\epsilon^+ - \epsilon)^2}} \frac{\epsilon^- - \epsilon'}{\sqrt{t^2 + (\epsilon^- - \epsilon')^2}} \\ \frac{\epsilon^+ - \epsilon}{\sqrt{t^2 + (\epsilon^+ - \epsilon)^2}} \quad \frac{t}{\sqrt{t^2 + (\epsilon^- - \epsilon')^2}} \end{pmatrix} \begin{pmatrix} \alpha_{k\sigma} \\ \beta_{k\sigma} \end{pmatrix}. \quad (2)$$

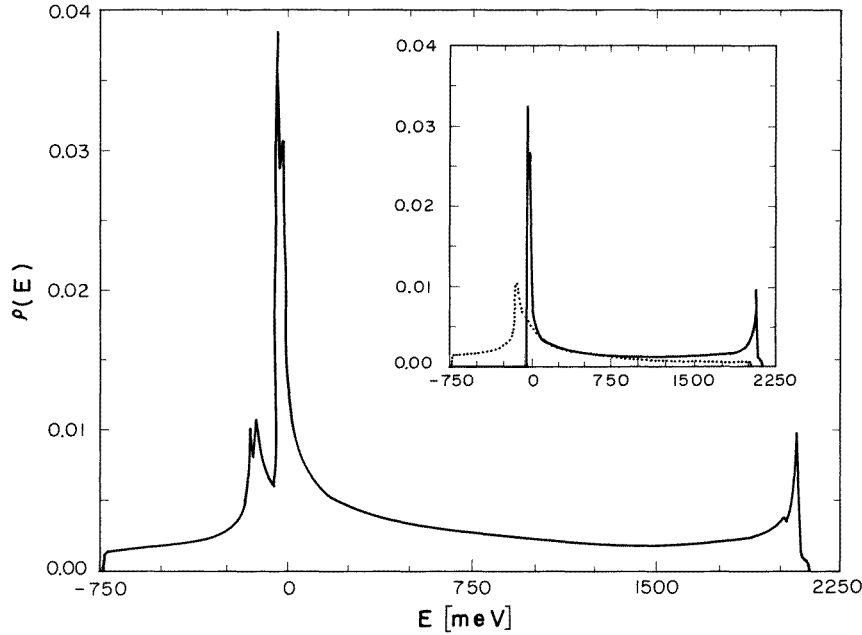


Figure 2. The DOS (in arbitrary units) for non-interacting quasiparticles is shown. The vHS is around 10 meV below the Fermi energy. The inset shows the partial DOS, where the dotted (solid) line corresponds to the ϵ^- -band (ϵ^+ -band).

The quasiparticles $\alpha_{k\sigma}^\dagger$ ($\beta_{k\sigma}^\dagger$) ‘live’ on the upper (lower) sheets of the FS given by $\epsilon^+ = 0$ ($\epsilon^- = 0$), where

$$\epsilon^\pm = \frac{1}{2}(\epsilon + \epsilon') \pm \sqrt{(\epsilon - \epsilon')^2 + 4t^2}$$

denote the dispersions of the two quasiparticle bands. Figure 1 shows the corresponding FS and figure 2 shows the partial and total density of states (DOS) with the van Hove singularities (vHS) predominantly located about 10 meV below the FS [15].

Superconductivity occurs through the interaction part of the Hamiltonian [11]:

$$H_I = -g \sum_{kk'} c_{k'\uparrow}^\dagger c_{-k'\downarrow}^\dagger c_{-k'\downarrow} c_{k\uparrow} - g' \sum_{kk'} d_{k'\uparrow}^\dagger d_{-k'\downarrow}^\dagger d_{-k'\downarrow} d_{k\uparrow} \\ + K \left(\sum_{kk'} d_{k\uparrow}^\dagger d_{-k'\downarrow}^\dagger c_{-k'\downarrow} c_{k\uparrow} + \text{HC} \right) \quad (3)$$

where g and g' are the pairing interactions (non-retarded) in the plane and chain respectively; K is the pairing interaction between the plane and chain electrons and is assumed repulsive. Interband coupling leads to the well known anticrossing feature in the band structure [13, 15] whenever two bands intersect. Consequently, the regions on the Fermi surface with pure plane or chain eigenstates are distinct and interband pairing is suppressed. It is this repulsive interaction that forces the quasiparticles in planes and chains away in real space, requiring

$$\sum_k \langle c_{k\sigma} d_{-k-\sigma} \rangle \simeq 0$$

which is a condition which demands that the pairing wave-function has nearly equal regions with positive and negative signs in the BZ. The origin of the intraband couplings could be phononic or electronic—it will not change the qualitative features of the results that follow, except that for phonon-mediated interaction we would have another energy scale: the cut-off frequency [11].

Application of a simple BCS mean-field theory followed by a transformation to the quasiparticle operators leads to a diagonalized mean-field Hamiltonian:

$$H_I^{mf} = \sum_k \Delta_k \alpha_{k\uparrow}^\dagger \alpha_{-k\downarrow}^\dagger + \sum_k \Delta'_k \beta_{k\uparrow}^\dagger \beta_{-k\downarrow}^\dagger + \text{HC} + \text{constant.}$$

Here,

$$\Delta_k = \frac{\Delta t^2 + \Delta'(\epsilon^+ - \epsilon)^2}{(\epsilon^+ - \epsilon)^2 + t^2} \quad \Delta'_k = \frac{\Delta' t^2 + \Delta(\epsilon^+ - \epsilon)^2}{(\epsilon^+ - \epsilon)^2 + t^2}$$

where

$$\Delta = -g \sum_k \langle c_{-k\downarrow} c_{k\uparrow} \rangle + K \sum_k \langle d_{-k\downarrow} d_{k\uparrow} \rangle$$

and

$$\Delta' = K \sum_k \langle c_{-k\downarrow} c_{k\uparrow} \rangle + g' \sum_k \langle d_{-k\downarrow} d_{k\uparrow} \rangle.$$

The two bands are completely decoupled now leading to the identification of Δ and Δ' as the gap functions in the plane and the chain respectively. On the FS, $\epsilon\epsilon' = t^2$ and one has a single order parameter:

$$\Delta_k = \Delta'_k = \frac{\Delta'\epsilon + \Delta\epsilon'}{\epsilon + \epsilon'}.$$

Since ϵ, ϵ' have the same sign on the FS, the only way that Δ_k can be made to change sign (and consequently have a node) along the FS is to have Δ and Δ' out of phase. This, of course, is ensured by the repulsive interaction K between the two bands; an attractive interband interaction would lead to the usual nodeless two-band superconductivity [11] with a modified density of states.

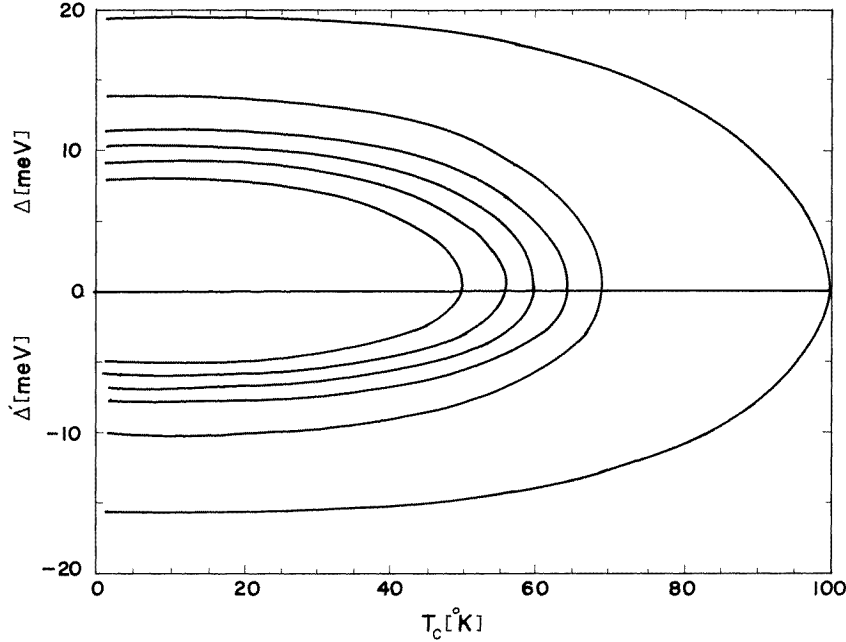


Figure 3. The self-consistent gap functions Δ, Δ' are plotted against temperature. The six different plots with increasing magnitudes of Δ are for $x = 0.5, 0.6, 0.7, 0.8, 0.9, 0.99$ respectively. Note that $\Delta\Delta' < 0$ for all of them.

The full Hamiltonian $H_0 + H_I^{mf}$ is diagonalized by using the Nambu representation $\psi_k^\dagger = (c_{k\uparrow}^\dagger, c_{-k\downarrow}^\dagger, d_{k\uparrow}^\dagger, d_{-k\downarrow}^\dagger)$ and writing the mean-field Hamiltonian as $\psi_k^\dagger \mathcal{M} \psi_k$, and the four eigenvalues are obtained from

$$2E_k^{\pm 2} = \eta + \eta' \pm \sqrt{(\eta - \eta')^2 + 4(\tau^2 + \delta^2)}$$

where

$$\begin{aligned} \eta &= \epsilon^2 + \Delta^2 + t^2 & \eta' &= \epsilon'^2 + \Delta'^2 + t^2 \\ \tau &= t(\epsilon + \epsilon') & \delta &= t(\Delta - \Delta'). \end{aligned}$$

The gap equations are solved numerically and the two gap functions have the usual square root dependence on temperature, but opposite signs (figure 3). This change of sign of the gap function on the same sheet of the FS has an important bearing on the physics of the model. The spectra E_k^\pm along different symmetry directions in the square Brillouin zone are plotted in figure 4(a), and show the anisotropy and the existence of a node in the gap. The corresponding DOS reflects the gapless behaviour (figure 4(b)) seen in tunnelling spectra as well. At low energies the DOS is linear in energy, as seen in various experiments—the

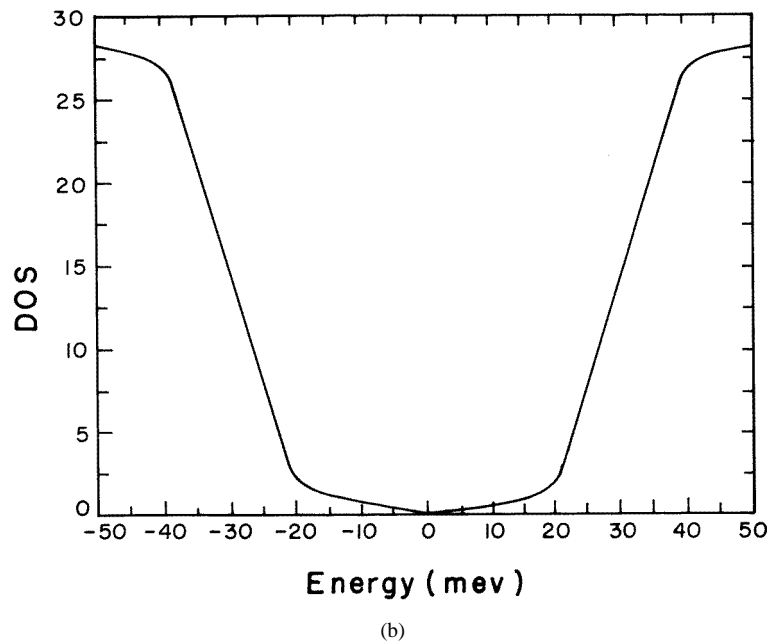
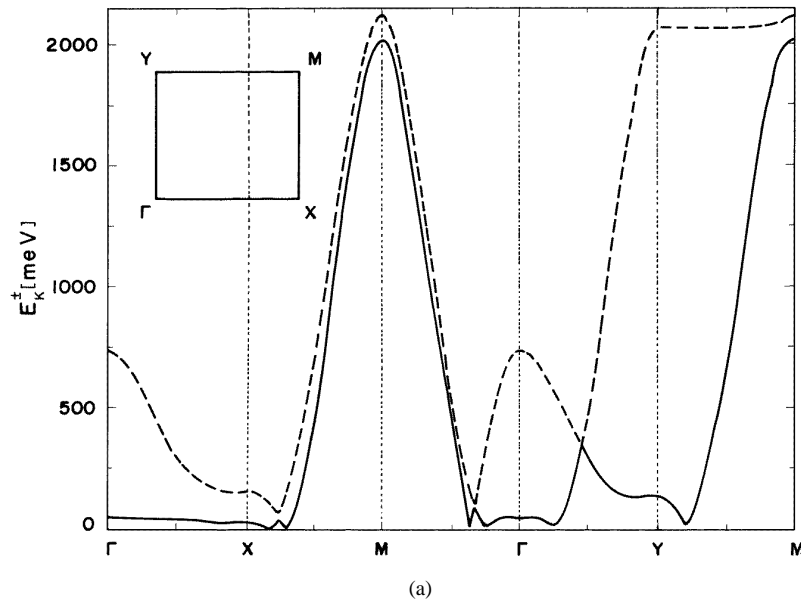


Figure 4. (a) The variation of the energy dispersion E_k^+ (E_k^-) along different symmetry directions of the first Brillouin zone (inset) of a square lattice is shown. In (b) the corresponding superconducting DOS (in arbitrary units) is plotted for low energies.

magnetic field dependence of the specific heat, the London penetration depth, tunnelling and a host of transport and thermodynamic properties.

The FS has contributions from the chain and plane bands and as we move along any one of the sheets of the FS the OP changes from Δ to Δ' (or vice versa), and hence changes

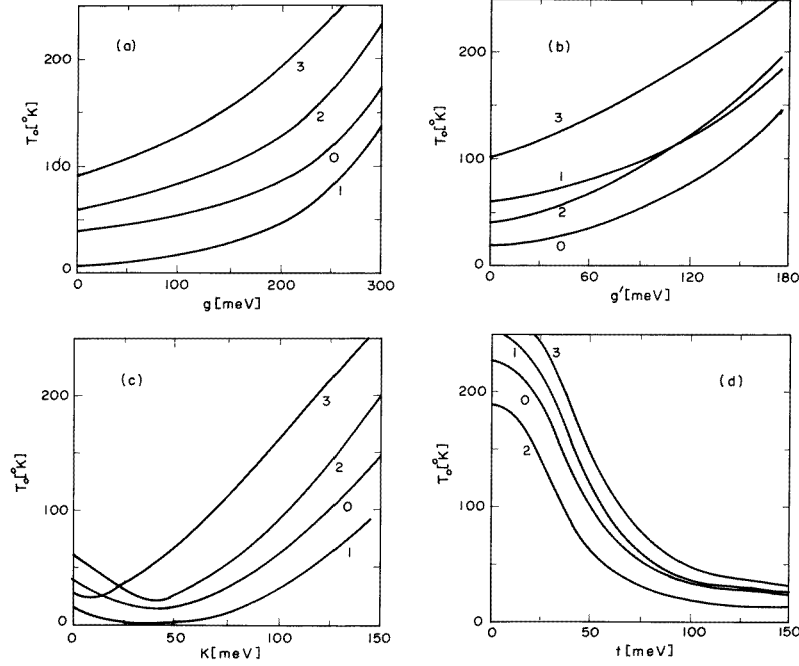


Figure 5. The figure shows how the mean-field T_c behaves with changes in the interaction parameters. (a) 0, 1, 2 and 3 are for the sets $\{g', K, t\} = \{140, 125, 50\}$, $\{100, 125, 50\}$, $\{140, 150, 50\}$ and $\{140, 125, 15\}$ respectively. (b) 0, 1, 2 and 3 are for the sets $\{g, K, t\} = \{225, 125, 50\}$, $\{275, 125, 50\}$, $\{225, 150, 50\}$ and $\{225, 125, 15\}$ respectively. (c) 0, 1, 2 and 3 are for the sets $\{g, g', t\} = \{225, 140, 50\}$, $\{225, 100, 50\}$, $\{275, 140, 50\}$ and $\{225, 140, 15\}$ respectively. (d) 0, 1, 2 and 3 are for the sets $\{g, g', K\} = \{225, 140, 125\}$, $\{250, 140, 125\}$, $\{225, 100, 125\}$ and $\{225, 140, 150\}$ respectively. The usual BCS-like variation of T_c with g and g' is observed in (a) and (b). The band interaction parameters K and t , however, affect T_c quite differently.

sign. This can be seen from an expansion of the mean-field free energy close to T_c to second order in Δ and Δ' :

$$F = a|\Delta|^2 + b|\Delta'|^2 + 4c(\Delta\Delta'^* + \text{HC}) \quad (4)$$

with

$$\begin{aligned} a &= \frac{g'}{gg' - K^2} - u - v - w \\ b &= \frac{g}{gg' - K^2} - u - v + w \\ c &= \frac{K}{gg' - K^2} + va \end{aligned} \quad (5)$$

where

$$u = \frac{1}{4} \sum_{\mathbf{k}} \left[\frac{\tanh \beta E^+(0, 0)}{E^+(0, 0)} + \frac{\tanh \beta E^-(0, 0)}{E^-(0, 0)} \right] \quad (6)$$

$$v = \frac{1}{2} \sum_{\mathbf{k}} \frac{t^2}{\sqrt{(\epsilon^2 - \epsilon'^2)^2 + 4t^2(\epsilon + \epsilon')^2}} \left[\frac{\tanh \beta E^+(0, 0)}{E^+(0, 0)} - \frac{\tanh \beta E^-(0, 0)}{E^-(0, 0)} \right] \quad (7)$$

and

$$w = \frac{1}{4} \sum_k \frac{\epsilon^2 - \epsilon'^2}{\sqrt{(\epsilon^2 - \epsilon'^2)^2 + 4t^2(\epsilon + \epsilon')^2}} \left[\frac{\tanh \beta E^+(0, 0)}{E^+(0, 0)} - \frac{\tanh \beta E^-(0, 0)}{E^-(0, 0)} \right]. \quad (8)$$

As $c \neq 0$, there is a single transition temperature— Δ and Δ' vanish simultaneously from opposite sides (figure 3); v is evidently positive and the optimal value of the repulsive interaction K always satisfies $K^2 < gg'$, so $c \geq 0$ (equality holds for $t = K = 0$). The free energy is then minimized with Δ and Δ' having opposite signs. This, of course, ensures that there is a node on the FS and that there is a single transition temperature and a single specific heat anomaly [2].

The positions of the nodes on the FS are shown in figure 1 for optimal values of g , g' and K (that fit T_c ; see the discussion below). The nodes are very close to the (π, π) direction as seen experimentally for $\text{YBa}_2\text{Cu}_3\text{O}_7$, a feature ascribed generally to the d-wave OP. The node positions obtained here are not very sensitive to the doping x (see the inset of figure 1) varying within $\pm 10^\circ$ about 45° . Although there are no experimental data to compare it with at present, this insensitivity remains a testable prediction of this model. For a d-wave OP, the node is completely insensitive to doping—fixed along the diagonal by symmetry.

The behaviours of T_c as a function of the interaction parameters g , g' and K and the interband hopping strength t are shown serially in the figures 5(a)–5(d). The variations of T_c with g and g' show the usual BCS behaviour. Interesting variations are observed in the dependence of T_c on K and t . As the two gap parameters Δ and Δ' have opposite signs, and t induces band mixing, T_c reduces quite dramatically with t . Conversely, K works counter to this, and pushes T_c higher, resulting in a minimum (that moves towards lower temperature as t is brought down from 50 to 15 meV) followed by the usual rise, as expected in a two-band model for superconductivity [11].

To obtain the superconducting transition temperature T_c as a function of the doping x in $\text{YBa}_2\text{Cu}_3\text{O}_{6+x}$ we have used as fitting parameters g , g' and K , while the band parameters have already been fixed to fit the ARPES data as discussed earlier. We chose values of these parameters such that g , g' and K are within reasonable limits, giving T_c at $x = 1$ around 100 K (figure 6). We have chosen a slightly higher value (100 K compared to the experimental value, $\simeq 90$ K) to account for the fluctuations that are present in these systems owing to their intrinsic low dimensionality. The optimal values of g , g' and K , thus fixed, turned out to be 225, 140 and 125 meV, with $t = 50$ meV fixed earlier. T_c is maximum at $x = 1$ where the Fermi level is closest to the vHS (figure 2). As the filling changes (controlled by the chemical potentials μ_p and μ_c), the DOS at the Fermi level drops drastically and then moves over a plateau. The T_c versus x curve (shown in figure 6) follows this pattern: the resemblance with the experimental curve for $\text{YBa}_2\text{Cu}_3\text{O}_{6+x}$ is noticeable.

We estimate the effects of fluctuation on the transition temperature following a method used earlier [16]. The method uses an elegant technique developed to calculate the superfluid density in the Hubbard model [17, 18]. The model studied here has a two-dimensional band coupled to a one-dimensional one. The coupling to the one-dimensional band introduces a $1/N$ effect and is negligible [19]. The relevant transition temperature is the Kosterlitz–Thouless (KT) temperature (T_{KT}). So T_{KT} serves as an upper limit and we neglect the one-dimensional couplings.

The superfluid density is calculated by minimally coupling a transverse vector potential (in a gauge $A_y = 0$) to the electrons by means of the usual Peierls phase factor. In the linear response, the current operator can be obtained by differentiating H_0 with respect to

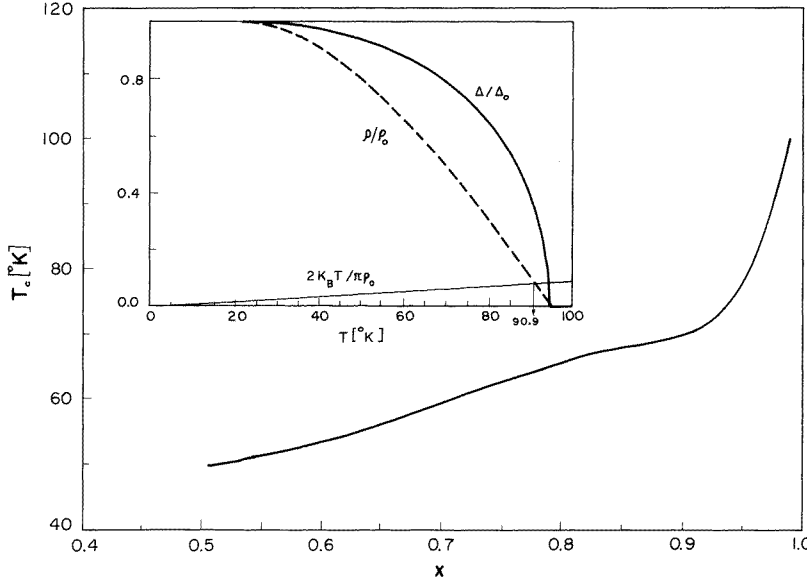


Figure 6. The plot shows the behaviour of T_c with doping concentration. The plateau around $x = 0.8$ and the maximum value of T_c appearing for $x \approx 1.0$ (because of the presence of vHS there). The inset shows the normalized superfluid density and gap function plotted as a function of temperature. ρ_0 is the superfluid density at $T = 0$. The KT transition temperature is shown by the arrow.

A_x :

$$j_x(r_i) = -c \frac{\partial H_0}{\partial A_x(r_i)} = j_x^{para} + j_x^{dia}. \quad (9)$$

The first term (j_x^{para}) is the paramagnetic contribution to the current, coming from the quasiparticle excitations above the condensate, and is of zeroth order in the vector potential. The term linear in A_x gives the diamagnetic current response, representing the screening of the Meissner condensate. The diamagnetic part is easily calculated to give

$$j_x^{dia} = -(ea/\hbar)^2 \frac{1}{Nc} \sum \langle \hat{n}_{k,\sigma} \rangle \frac{\partial^2 \epsilon_k}{\partial k_x^2} A_x(\mathbf{q}). \quad (10)$$

The diamagnetic superfluid density is thus proportional to the average electronic kinetic energy in the x -direction [17]. Only in the case of a parabolic DOS will it become proportional to the usual average electronic density.

The paramagnetic part of the current can be found using linear response theory, and in the long-wavelength, static limit

$$j_x^{para} = -c^{-1} \left[\lim_{q \rightarrow 0} \lim_{\omega \rightarrow 0} \Lambda_{xx}(\mathbf{q}, \omega) \right] A_x(\mathbf{q}) \quad (11)$$

where

$$i\Lambda_{xx}(\mathbf{q}, \omega) = \int dt \theta(t) \exp(i\omega t) \langle [j_x^{para}(\mathbf{q}, t), j_x^{para}(-\mathbf{q}, 0)] \rangle. \quad (12)$$

The correlation function above is easily calculated for the model in hand, with averages calculated in the mean-field ground state:

$$\rho_s(T) = (2Na^2)^{-1} \sum_k \left[f'(E_k) \left(\frac{\partial \epsilon_k}{\partial k_x} \right)^2 + \frac{1}{2} g(k) \frac{\partial^2 \epsilon_k}{\partial k_x^2} \right] \quad (13)$$

where

$$g(k) = 1 - \frac{\epsilon_k - \epsilon_F}{E_k} \tanh \frac{E_k}{2KT}.$$

The normalized superfluid density $\rho_s(T)/\rho_s(0)$ is plotted in the inset in figure 6 against temperature. It has the usual shape and vanishes at the mean-field transition temperature as expected. The KT transition temperature T_{KT} is characterized by a discontinuous jump in ρ_s , and this temperature is obtained from the well known relation

$$\frac{\pi}{2} \rho_s(T) = K_B T$$

at $T = T_{KT}$. Note that even though the jump in ρ_s is obtained only when we include the renormalization (due to the vortex-like fluctuation) of the order parameters, the procedure used here is known to give a good estimate of T_{KT} [18]. We have chosen to work in a particular gauge and, in order to make the calculations gauge invariant, it is necessary to consider vertex corrections.

The intersection of the straight line with ρ_s (see the inset in figure 6) gives the value of the transition temperature, and a reduction from the mean-field value by about five per cent is noticed. The optimal values of the parameters K , g , g' above have been chosen in such a way that this reduction is accounted for and the reduced T_c turns out to be around 90 K at $x = 1$, as is the case for YBCO.

3. Conclusions

The two order parameters in our model are not related by any symmetry; they have different signs. The c -axis Josephson current, therefore, does not cancel out completely as in a d -wave superconductor, although partial cancellation occurs due to the opposite signs of Δ and Δ' , resulting in a small (compared to that for an s -wave OP) but finite current [9, 20]. The node on the FS is close to the (π, π) direction, and not very sensitive to doping. Recent microwave measurements on very high-quality YBCO single crystals [21] are consistent with a multicomponent order parameter, though it is not yet clear whether this involves multiple transition temperatures. The OP in the a -direction (b -direction) is mainly chain-like (plane-like) and provides a natural explanation for the observed phase change, of π , in SQUID experiments. An s -wave superconductor is weakly influenced by impurities (the Anderson theorem), while in a d -wave superconductor, scattering between lobes of different signs on the FS has a drastic effect. This averaging out of the sign and the consequent sensitivity of T_c to non-magnetic impurities will arise in the present model as well, albeit at a much lower rate than in the d -wave case. The sign of the OP changes in the present model only as a result of scattering from planes to chains—involving strong, large-momentum scattering processes only. The sensitivity of T_c to non-magnetic impurity will, therefore, be intermediate between that of an s -wave superconductor and that of a d -wave superconductor here [20], a feature seen in the high- T_c materials [2, 9]. Leading-order two-dimensional fluctuations do not seem to alter the phase diagram very much, just pushing the critical line down by a few degrees. At low energies the SDOS is linear in energy. This feature, along with the presence of nodes, ensures that the thermodynamic

properties are non-activated, and they show a power-law dependence on temperature, as seen in various experiments including ones that investigate the magnetic field dependence of the specific heat, the London penetration depth, tunnelling and other thermodynamic and transport properties. The London penetration depth turns out to be anisotropic, a feature easily derived from the anisotropy of E_k in the Brillouin zone (figure 4(b)).

The conclusions of the present model are not very sensitive to whether we work with a chain and a plane, two or more planes (or chains), or a combination of these. This is a simple model that incorporates the effect of more than one OP residing on different coupled bands. We have shown that, with the correct choice of the phases of the different OP, this model can capture many of the unusual features of the symmetry of the OP in these systems. Even in the case of monolayer systems, there remains the possibility of coupled bands, and hence different OPs residing on different bands. Note that, unlike the model of Yakovenko [22], the present model gives rise to a situation where the OP changes sign on *both of the sheets of the FS* as one moves along the FS. It would be nice to see experimental results on the position of the node(s) on the FS with doping. The node position is dictated by symmetry in the d-wave case, independently of the shape of the FS, while in any of the s-wave models, it changes with the doping. As shown here, even a simple model that incorporates multiple, coupled order parameters can capture a lot of unusual experimental signatures regarding the symmetry of the OP for the high- T_c cuprates. Any conclusions, based on any model, that seem to ‘explain’ part of the story, are therefore going to be premature: a lot of work, both experimental and theoretical, needs to be done before any firm consensus emerges.

References

- [1] Shen Z X *et al* 1993 *Phys. Rev. Lett.* **70** 1553
- [2] Annet J, Goldenfeld N and Leggett A J 1996 *Physical Properties of High Temperature Superconductors* vol 5, ed D M Ginsberg (Singapore: World Scientific)
Sigrist M and Ueda K 1991 *Rev. Mod. Phys.* **63** 239
Dynes R C 1994 *Solid State Commun.* **92** 53
- [3] Hardy W N, Bonn D A, Morgan D C, Liang Ruixing and Zhang Kuan 1993 *Phys. Rev. Lett.* **70** 3999
Sonier J E *et al* 1994 *Phys. Rev. Lett.* **72** 744
- [4] Campuzano J P *et al* 1990 *Phys. Rev. Lett.* **64** 2308
- [5] Wollman D A, van Harlingen D J, Lee W C, Ginsberg D M and Leggett A J 1993 *Phys. Rev. Lett.* **71** 2134
van Harlingen D J 1995 *Rev. Mod. Phys.* **67** 515
- [6] Tsuei C C, Kirtley J R, Chi C C, Yu-Jahnes L S, Gupta A, Shaw T, Sun J Z and Katchen M B 1994 *Phys. Rev. Lett.* **73** 594
- [7] Sun A G, Gajewski D A, Maple M B and Dynes R C 1994 *Phys. Rev. Lett.* **72** 2267
- [8] Chaudhari P and Lin S-Y 1994 *Phys. Rev. Lett.* **72** 1084
- [9] Sun A G, Paulius L M, Gajewski D A, Maple M B and Dynes R C 1994 *Phys. Rev. B* **50** 3266
- [10] Annet J, Goldenfeld N and Renn S R 1991 *Phys. Rev. B* **43** 2778
Schrieffer J R 1994 *Solid State Commun.* **92** 129
- [11] Suhl H, Matthias B T and Walker R L 1959 *Phys. Rev. Lett.* **3** 552
- [12] Combescot R and Leyronas X 1995 *Phys. Rev. Lett.* **75** 3732
- [13] Yu Jaejun, Massidda S, Freeman A J and Koeling D D 1987 *Phys. Lett.* **122A** 203
Pickett W E, Krakauer H, Cohen R E and Singh D J 1992 *Science* **255** 46
- [14] Fehrenbacher R and Norman M 1995 *Phys. Rev. Lett.* **74** 3884
- [15] Gofron K, Campuzano J C, Ding H, Gu C, Liu R, Dabrowski B, Veal B W, Cramer W and Jennings G 1994 *J. Phys. Chem. Solids* **54** 1193
- [16] Chattopadhyaya B, Gaitonde D M and Taraphder A 1996 *Europhys. Lett.* **34** 705
- [17] Scalapino D J, White S R and Zhang S C 1992 *Phys. Rev. Lett.* **68** 2830
- [18] Denteneer P J H, An G and van Leeuwen J M J 1991 *Europhys. Lett.* **16** 5
- [19] The authors acknowledge helpful discussion with C Dasgupta on this point.

- [20] Mohanty P K and Taraphder A 1996 *Preprint* cond-mat/9603180
Mohanty P K and Taraphder A 1996 *Ten Years After the Discovery of High Temperature Superconductors* ed
K B Garg (India: Narosa)
- [21] Srikanth H, Willemsen B A, Jacobs T, Sridhar S, Erb A, Walker E and Flukiger R 1997 *Phys. Rev. B* **55**
14 733
- [22] Yakovenko V 1995 *Phys. Rev. Lett.* **75** 4135